give rise to channel correlation and reduction of MIMO capacity. To suppress PIFAs' in-band coupling, a tunable parasitic element is custom designed and incorporated on the handheld chassis to follow the operation frequency of the PIFAs. Measurement results confirm that the parasitic element can be tuned to effectively suppress PIFA coupling by more than 10 dB in the entire tuning range from LTE13 to GSM900. MIMO system calculations also confirm the efficacy of the employed technique in improving channel capacity close to that of an uncorrelated system.

ACKNOWLEDGMENT

The authors would like to thank Dr. S. Ali of Research in Motion Ltd. for her insightful comments and also Mr. D. Wang of Research in Motion Ltd. for fabrication of the prototypes.

REFERENCES

[1] J. R. De Luis, A. Morris, G. Qizheng, and F. De Flaviis, "Tunable antenna systems for wireless transceivers," in *Proc. IEEE Int. Symp. on Antennas and Propagation (APSURSI)*, Jul. 2011, pp. 730–733.

[2] J.-H. Lim, Z.-J. Jin, and T.-Y. Yun, "A frequency reconfigurable PIFA using a PIN diode for mobile-WiMAX applications," in *Proc. IEEE MTT-S Int. Microwave Workshop Series on Intelligent Radio for Future Personal Terminals*, Aug. 2011, pp. 1–2.

[3] L. M. Feldner, C. T. Rodenbeck, and C. G. Christodoulou, "Tunable electrically small UHF PIFA-as-a-package," in *Proc. IEEE Antennas and Propagation Society Int. Symp.*, Jul. 2006, pp. 185–188.

[4] G. McFeetors and M. Okoniewski, "Performance and operation of stressed dual gap RF MEMS varactors," in *Proc. 36th Eur. Microwave Conf.*, September 2006, pp. 1064–1067.

[5] J. Sarrazin, Y. Mahe, S. Avrillon, and S. Toutain, "Four colocated antennas for MIMO systems with a low mutual coupling using mode confinement," in *Proc. IEEE Antennas and Propagation Society Int. Symp.*, Jul. 2008, pp. 1–4.

[6] A. C. K. Mak, C. R. Rowell, and R. D. Murch, "Isolation enhancement between two closely packed antennas," *IEEE Trans. Antennas Propag.*, vol. 56, no. 11, pp. 3411–3419, Nov. 2008.

[7] K. Payandehjoo and R. Abhari, "Investigation of parasitic elements for coupling reduction in multi-antenna hand-set devices," *Int. J. RF and Microw. Comput.-Aided Engrg.*, Jan. 2013 [Online]. Available: http://onlinelibrary.wiley.com/doi/10.1002/mmce.20706/abstract

[8] E. Saenz, K. Guven, E. Ozbay, I. Ederra, and R. Gonzalo, "Decoupling of multifrequency dipole antenna arrays for microwave imaging applications," *Int. J. Antennas Propag.*, vol. 2010, p. 8, 2010.

[9] Z. Li, Z. Du, M. Takahashi, K. Saito, and K. Ito, "Reducing mutual coupling of MIMO antennas with parasitic elements for mobile terminals," *IEEE Trans. Antennas Propag.*, vol. 60, no. 2, pp. 473–481, Feb. 2012.

[10] M. A. Jensen and Y. Rahmat-Samii, "Performance analysis of antennas for hand-held transceivers using FDTD," *IEEE Trans. Antennas Propag.*, vol. 42, no. 8, pp. 1106–1113, Aug. 1994.

Loop-Type Ground Radiation Antenna for Dual-Band WLAN Applications

Yang Liu, Hyung-Hoon Kim, and Hyeongdong Kim

***Abstract*—A compact ground radiation method for 2.45 and 5.5 GHz wireless local area network (WLAN) applications is proposed. This method is based on two different loop-type current modes that are excited in the ground plane and separately operated at 2.45 and 5.5 GHz, producing a very small-sized antenna with good radiation efficiencies and wide impedance bandwidths. The proposed radiation method requires a small ground clearance of 8.5 mm $\times$ 4.5 mm for installing the antenna element. The experimental result shows that a good impedance matching performance is simultaneously achieved at the dual frequency bands and the -10 dB bandwidths are obtained as 120 MHz and 720 MHz at the 2.45 and 5.5 GHz frequency bands, respectively, and good radiation performance is achieved.**

***Index Terms*—Ground radiation antenna, loop-type current, loop feed, dual-band, wireless local area network (WLAN).**

I. INTRODUCTION

Wireless local area network (WLAN), also known as wireless fidelity (Wi-Fi), remains one of the fastest growing areas of data communication and is rapidly increasing in importance. Recently, dual-band antennas operating in the 2.4 and 5 GHz (IEEE 802.11b/g and IEEE 802.11a) WLAN bands have been used to resolve congestion in the 2.4 GHz bandwidth in order to meet the rapidly rising market demand for faster data rates. Despite abundant research on mobile antennas, which has focused on providing sufficient bandwidth to simultaneously cover the 2.45 and 5.5 GHz frequency bands [1]–[8], all existing approaches require large ground clearance to install the antenna element, which is a critical limitation of modern mobile handsets.

Reducing the available space in mobile devices requires smaller antenna elements, threatening antenna performance in terms of the impedance bandwidth and efficiency. To address this challenging issue, an innovative radiation method known as a ground radiation antenna (GradiAnt) was presented in [9]–[12]. Unlike the conventional quarter wavelength inverted-F antenna (IFA), the ground radiation method requires a very small ground clearance with lumped capacitors, which produces a large loop-type currents formed in the ground plane. The ground radiating current mode [13], [14] can be strongly coupled if the loop-type currents are close to the magnetic field maximum of the ground plane such that it is able to provide a wide impedance bandwidth. However, the GradiAnt presented in previous studies only provides a single band operation, which cannot meet the market requirements of modern communications. In this communication, we modify the feed structure for exciting the antenna in order to meet the dual-band WLAN communication requirement, in which two different loop-type current modes operated at 2.45 and 5.5 GHz are simultaneously excited in the ground plane. With the proposed radiation

Manuscript received November 13, 2012; revised April 15, 2013; accepted June 03, 2013. Date of publication June 11, 2013; date of current version August 30, 2013. This work was funded by the Ministry of Science, ICT & Future Planning (MSIP), Korea in the ICT R&D Program 2013.

Y. Liu and H. Kim are with the Department of Electronics and Computer Engineering, Hanyang University, Seoul, Korea (e-mail: hdkim@hanyang.ac.kr).

H.-H. Kim is with the Department of Biomedical Engineering, Kwangju Women's University, Kwangju, Korea.

Color versions of one or more of the figures in this communication are available online at http://ieeexplore.ieee.org.

Digital Object Identifier 10.1109/TAP.2013.2267716

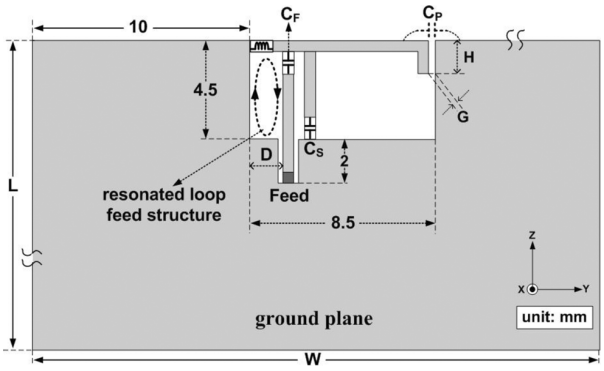

Fig. 1. Configuration of dual-band ground radiation antenna.

method, the antenna only occupies a very small space of 8.5 mm × 4.5 mm, approximately $0.07\lambda \times 0.04\lambda$ and $0.15\lambda \times 0.08\lambda$ at 2.45 and 5.5 GHz, respectively. This is different from other loop antennas [15], [16], which require half-wavelength and one-wavelength structures to achieve multiband operation. Since the loop-type currents just act as coupling elements that couple the ground radiating modes, the radiation performance can be very dependent upon the size or the shape of the ground plane. We report our investigation of the variations in the radiation characteristics with different sizes of the ground plane.

II. Antenna Configuration

As shown in Fig. 1, a compact GradiAnt structure is placed in a ground clearance that measures 8.5 mm × 4.5 mm. The 100 mm × 50 mm (L × W) ground plane, which is the size used in modern mobile handsets, is printed on a 0.8 mm-thick FR4 substrate ($\varepsilon_r = 4.4$). A resonated loop feed structure [17], including a capacitor C_F (0.19 pF) and an inductor (0.8 nH), is used in order to drive the antenna to create two different loop-type current modes in the ground plane. The first loop, operated at 2.45 GHz, is formed by the ground plane connected by an inductor and a distributed capacitor C_P, which is coupled by the resonated loop feed structure. The second loop, operated at 5.5 GHz, is formed by the feed conductor, top-conductor, C_P and the ground plane and is coupled by C_F. An additional coupling capacitor C_S (0.17 pF) is placed 0.5 mm away from the feed conductor and plays an important role in controlling the input impedance at the 5.5 GHz frequency band. For practical application in the mobile handset industry, a 2 mm-long transmission line is used in order to connect a typical 50 Ω RF switch connector usually installed in the PCB. The other parameters are D = 1.5, G = 0.3, and H = 1.5 mm. All antenna simulations in this communication were performed using Ansoft HFSS.

III. Antenna Tuning Mechanisms and Results

A. Impedance-Controlling Technique

The input impedance in the lower band is determined by the area of the resonated loop feed structure. It also can be controlled by C_F without changing the area of the feed structure. However, the input impedance in the higher band is also influenced by C_F, resulting in a difficulty in achieving simultaneously matched impedance at the dual frequency bands [18]. To solve this problem, a shunt capacitor, C_S, is used. Since the loop-type current mode operated at 5.5 GHz is electrically coupled by C_F, the amount of charge on the top conductor is compactly accumulated close to C_F. Under the condition that the value of C_F is unchanged, these charges can be divided between C_F and C_S, resulting in a weak electric coupling and hence a changed mutual impedance between the feed structure and the radiator. Thus, the input impedance at the higher band can be conveniently controlled by varying C_S.

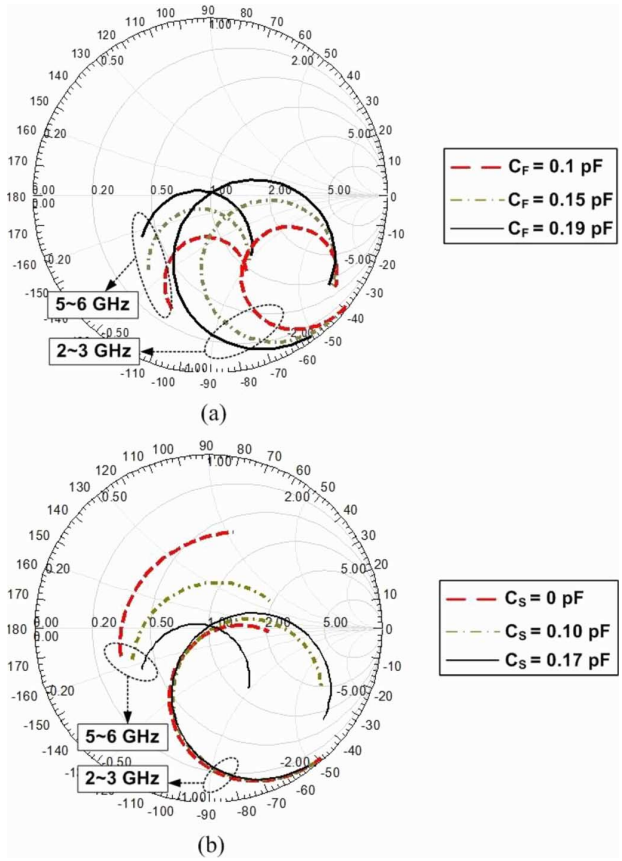

Fig. 2. Simulated input impedance with (a) different C_F and (b) different C_S on Smith Chart.

Simulations were conducted to demonstrate the impedance variation that occurs when C_F and C_S vary. It is clear from Fig. 2(a) that the input impedance of both the frequency bands (2–3 GHz and 5–6 GHz) can be controlled by varying C_F. As shown in Fig. 2(b), when C_S is 0 pF, the GradiAnt presents a large impedance mismatch in the higher band and only provides a single band operation at the lower band. As the ground clearance size becomes smaller compared to that (15 mm × 5 mm) of the dual-band IFA presented in [17], the area of the loop-type current operated at the higher band decreases and the impedance mismatch effect can be attributed to the significantly reduced real part of the input impedance. This effect occurs frequently with conventional monopoles [19]. As C_S increases to 0.17 pF, it results in a well-matched impedance antenna that is able to provide sufficient bandwidth at the higher band. Note that the input impedance in the lower band is almost unchanged when C_S varies. This is important to achieve simultaneously matched impedance in the dual frequency bands.

B. Frequency-Controlling Technique

Fig. 3 shows the simulated normalized surface current density. It is clear from Fig. 3(a) and (b) that the two different loop-type current modes are excited at 2.45 and 5.5 GHz and each loop is connected by the distributed capacitor C_P. Thus, the resonant frequencies of the two loops can be controlled by C_P [9], [11], which can be adjusted via the parameter H or G, as shown in Fig. 1. As shown in Fig. 4(a), when C_P

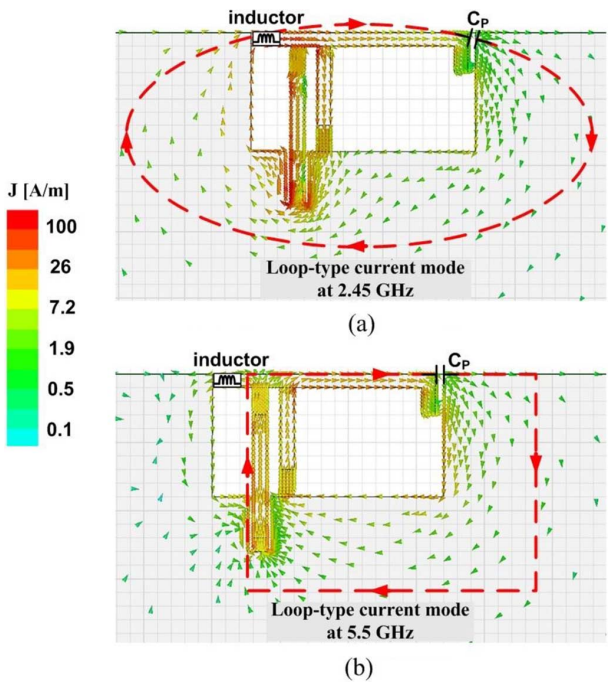

Fig. 3. Computed normalized surface current density showing two different loop modes at (a) 2.45 and (b) 5.5 GHz.

increases, (increasing H from 1 to 2 mm), the resonant frequencies are lowered from 2.5 to 2.38 GHz and from 5.87 to 5.21 GHz.

Like in the input impedance controlling method, the resonant frequency of one loop should be able to be maintained when controlling the resonant frequency of the other. This would be easy for antenna tuning. As can be seen from Fig. 3, the inductor is included in the current loop at 2.45 GHz, but is not included in the current loop at 5.5 GHz. This is because the impedance of the resonated loop feed structure at 5.5 GHz becomes larger than that at 2.45 GHz, resulting in the current flowing through the inductor at 5.5 GHz being much weaker than that at 2.45 GHz. This can be observed from Fig. 3(b). Therefore, the inductor plays an important role in controlling the resonant frequency at the lower band while maintaining the resonant frequency at the higher band. As demonstrated in Fig. 4(b), when the inductor is changed from 0.4 to 1.2 nH, the resonant frequency varies from 2.54 to 2.36 GHz, while the resonant frequency at the 5.5 GHz frequency band is unchanged.

What should be mentioned here is that C_S also has an effect of lowering the resonant frequencies because it is connected in parallel to the distributed capacitor C_P. Fig. 5 shows the simulated and measured reflection coefficient of the GradiAnt. When the path of C_S is removed from the feed structure, the loop mode at the 5.5 GHz frequency band disappears due to the large impedance mismatch, and the GradiAnt only provides a single band operation at 3 GHz. Based on the contribution of C_S, the hidden mode at the 5.5 GHz frequency band is revived, and the -10 dB impedance bandwidths are obtained as 120 MHz (2.39–2.51 GHz) and 720 MHz (5.15–5.87 GHz) at 2.45 and 5.5 GHz, respectively. The measured result substantiates the simulation result. Table I shows the measured efficiencies and peak gains at the dual frequency bands.

Fig. 6 shows the measured radiation patterns. On the *xz*-plane, the antenna produces omni-directional patterns for the E-phi component at both 2.45 and 5.5 GHz. On the *xy*-plane, the patterns for the theta and phi components are symmetrical at both 2.45 and 5.5 GHz. These radiation patterns indicate that a dipole-type radiating current mode is generated along the y-axis of the ground plane due to magnetic coupling from the two loop-type current modes.

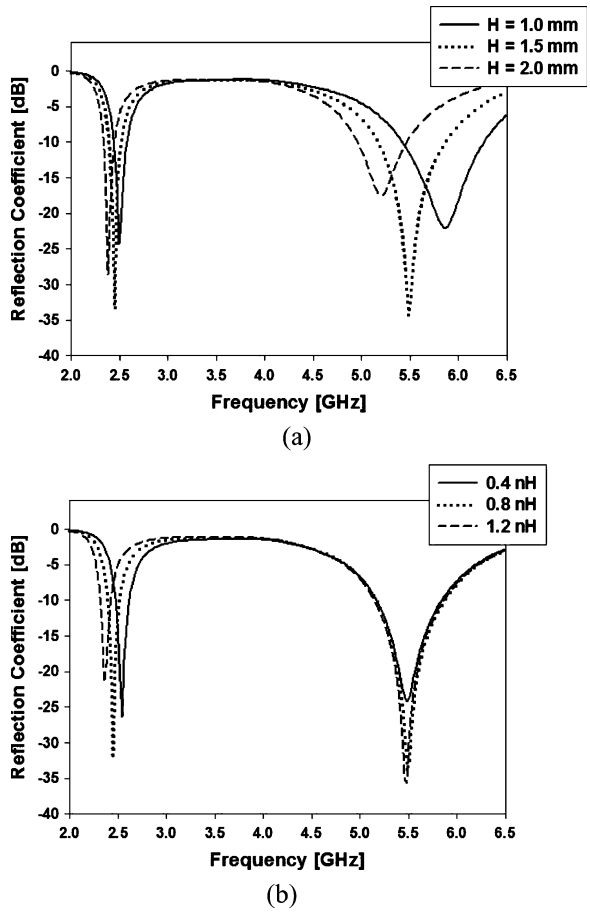

Fig. 4. Resonant frequency variations with (a) different C_P and (b) different inductor.

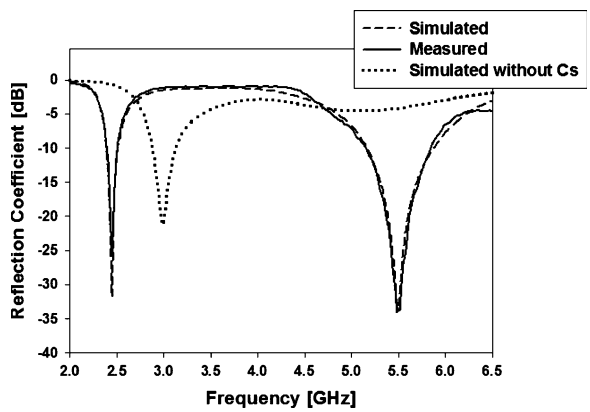

Fig. 5. Simulated and measured reflection coefficient of the proposed antenna.

TABLE I
MEASURED ANTENNA EFFICIENCIES AND PEAK GAINS

Frequency (GHz)	2.40	2.45	2.50	5.15	5.35	5.70	5.85
Efficiency (%)	70.5	71.6	70.2	69.1	70.2	71.7	71.2
Peak gain (dBi)	2.03	2.12	2.07	1.68	1.75	1.63	1.66

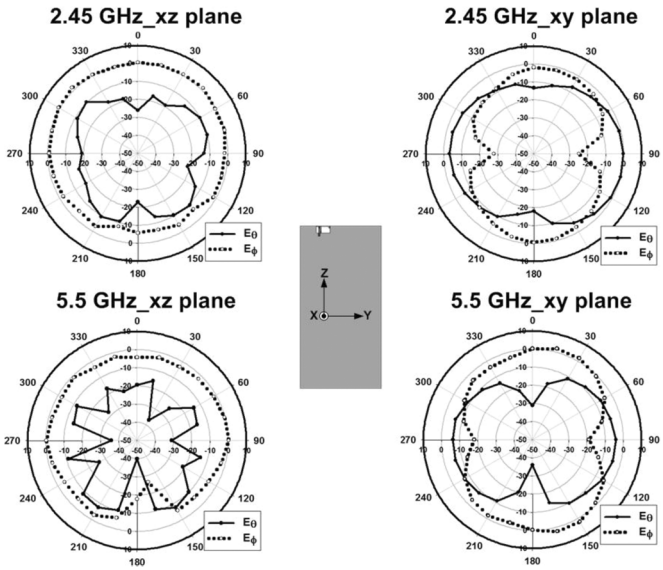

Fig. 6. Measured radiation patterns of the proposed antenna.

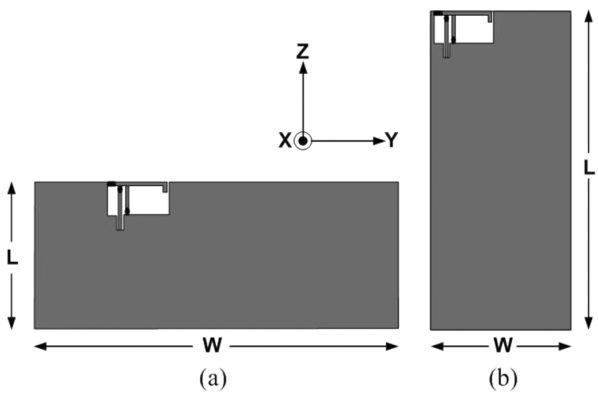

Fig. 7. (a) Reducing ground length L to 20 mm, and (b) reducing ground length L and width W to 50 and 20 mm, respectively.

IV. Discussion of Effect of Ground Size

Investigation of the effect of the ground plane size on radiation performance of the GradiAnt is studied in this section. Because the loop-type current modes produced by the antenna are formed in the ground plane, the resonant frequency and the input impedance can be changed as the size of the ground plane varies. An advantage of the proposed antenna is that it allows for the resonant frequency to be conveniently controlled by C_P and the inductor, and that the input impedance can be conveniently adjusted by C_F and C_S. Therefore, the antenna tuning can be completed without changing the antenna structure. The maximum impedance bandwidth, however, is difficult to achieve by adjusting the matching components, and is directly determined by the coupling between the antenna resonant modes and the dipole-type radiation modes of the ground plane [13], [20], which depends on the ground size, antenna size, and the position of the antenna in the ground plane.

The effects of the ground plane on impedance bandwidth and radiation patterns are studied using two different ground planes. The first, as shown in Fig. 7(a), reduces L to 20 mm while maintaining W as 50 mm. The second, as shown in Fig. 7(b), reduces L and W to 50 mm and 20 mm, respectively, and places the antenna at the corner of the ground plane. Fig. 8 shows the simulated reflection coefficients of the antenna with the two different ground planes. By using the impedance

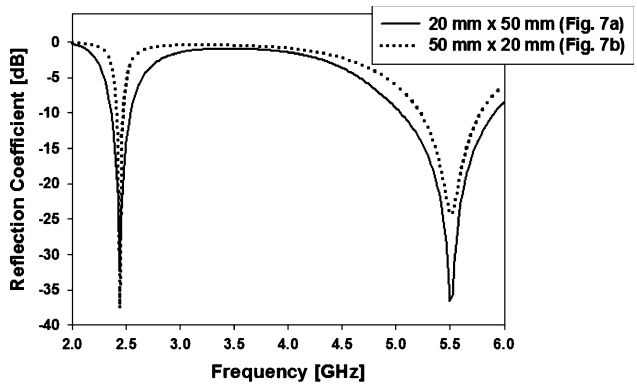

Fig. 8. Comparison of impedance bandwidths produced by two different ground planes.

and frequency controlling techniques described in Section III, it is clear that both cases achieve simultaneously well-matched impedance at 2.45 and 5.5 GHz, but the impedance bandwidths of the two cases are quite different. The 20 mm × 50 mm ground plane (Fig. 7(a)) achieves the −10 dB bandwidth as 180 MHz (2.36–2.54 GHz) and 870 MHz (5.05–5.92 GHz) at the dual frequency bands. On the other hand, the −10 dB bandwidth is simulated as 60 MHz (2.41–2.47 GHz) and 550 MHz (5.23–5.78 GHz) for the second case (Fig. 7(b)).

As mentioned in the case of the 100 mm × 50 mm ground plane, the dipole-type radiating current modes along the y-axis of the ground plane are coupled mostly through magnetic coupling from the loop-type current modes. The coupling can be enhanced by reducing the length of the ground plane. This is because the radiating currents flowing along the y-axis of the ground plane can be concentrated close to the loop-type current modes as L reduces, resulting in a strong magnetic coupling. As a result, when the ground plane is 20 mm × 50 mm, the bandwidths in both the frequency bands are even larger than that produced by the 100 mm × 50 mm ground plane. The coupling can be significantly reduced when the antenna is placed at the corner as shown in Fig. 7(b), which may produce the worst radiation performance. Since the antenna is located close to the electric field maximum of the ground plane, the loop-type antenna mode is not proper to act as the coupling element and the IFA-type antennas can be used in order to achieve the optimal coupling in this case [17]. Naturally, the antenna size needs to be increased when IFA antennas are used.

Fig. 9 shows the simulated radiation patterns produced by the two different ground planes. For the 20 mm × 50 mm ground plane, as shown in Fig. 9(a), good omni-directional performance was obtained for E-phi component on the *xz*-plane at both 2.45 and 5.5 GHz, similar to the results measured by the 100 mm × 50 mm ground plane. This response is as expected, the dipole-type radiating current modes along the y-axis of the ground plane are not changed as the length of the ground plane reduces. For the 50 mm × 20 mm ground plane, as shown in Fig. 9(b), the omni-directional pattern was still observed on the *xz*-plane at 5.5 GHz, but it changed at 2.45 GHz. As the width of the ground plane is reduced less than the half wavelength of 2.45 GHz, the dipole-type radiating current mode along the y-axis cannot be excited, and the radiating current mode along the z-axis can be coupled by the antenna, producing omni-directional pattern for E-theta component on the *xy*-plane. Table II compares the relative bandwidths obtained by different sizes of the ground plane and ground clearance. It is shown that the ground clearance size of the proposed antenna is reduced by up to 49% compared to the former work [17] and the relative bandwidths at 2.45 and 5.5 GHz are only reduced by 1.2% and 9.1%, respectively. Note that the proposed antenna with the 20 mm × 50 mm ground plane

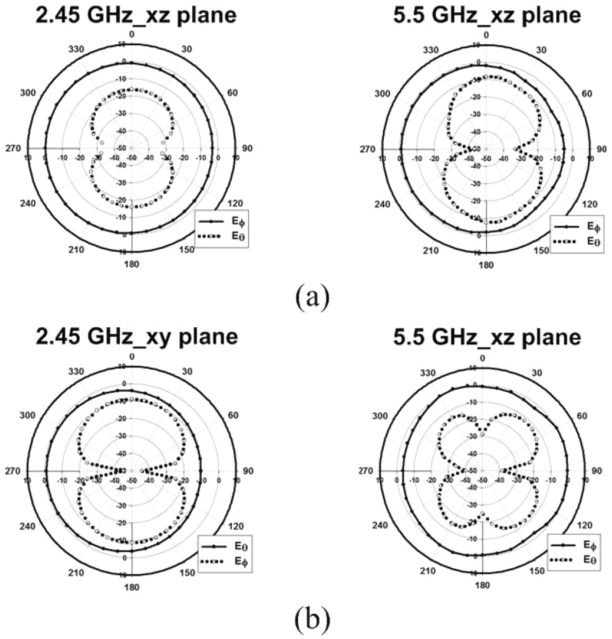

Fig. 9. Simulated radiation patterns produced by (a) 20 mm (L) × 50 mm (W) ground plane and (b) 50 mm (L) × 20 mm (W) ground plane.

TABLE II
COMPARISON OF RELATIVE BANDWIDTHS OBTAINED BY DIFFERENT SIZES OF THE CLEARANCE AND GROUND

antenna design	Fig. 1	Fig. 7a	Fig. 7b	PIFA [17]
clearance (mm)	8.5 × 4.5			15 × 5
ground plane L × W (mm)	100 × 50	20 × 50	50 × 20	45 × 20
-10 dB bandwidth (%)	2.45 GHz			
	4.9	7.3	2.4	6.1
	5.5 GHz			
	13.1	15.8	10	22.2

produces an even larger bandwidth at 2.45 GHz than that obtained by the PIFA in the former work.

V. CONCLUSION

In this communication, a loop-type ground radiation antenna with a modified feed structure has been proposed. The proposed antenna successfully achieved dual-band operation by exciting two different loop-type current modes formed in the ground plane, separately operated at the 2.45 and 5.5 GHz frequency bands. With a small antenna size, the feed structure modified using an additional shunt capacitor resulted in an optimized impedance matching performance, and the achieved impedance bandwidths fully cover the WLAN communication bands. The investigation of the variations in the radiation characteristics with different sizes of the ground plane was also studied in this communication. The wide impedance bandwidths at dual frequencies can be achieved by enhancing the coupling between the loop-type current modes and the ground radiating current modes, even though the antenna element is small.

ACKNOWLEDGMENT

The authors would like to thank RadiNa Inc. Ltd., Korea, for manufacture and measurement support.

REFERENCES

[1] Y. L. Kuo and K. L. Wong, "Printed double-T monopole antenna for 2.4/5.2 GHz dual-band WLAN operation," *IEEE Trans. Antennas Propag.*, vol. 51, no. 9, pp. 2187–2192, Sept. 2003.
[2] K. L. Wong, L. C. Chou, and C. M. Su, "Dual-band flat-plate antenna with a shorted parasitic element for laptop applications," *IEEE Trans. Antennas Propag.*, vol. 53, no. 1, pp. 539–544, Jan. 2005.
[3] Y. S. Wang, M. C. Lee, and S. J. Chung, "Two PIFA-related miniaturized dual-band antennas," *IEEE Trans. Antennas Propag.*, vol. 55, no. 3, pp. 805–811, Mar. 2007.
[4] S. J. Jeong and K. C. Hwang, "Compact loop-coupled spiral antenna for multiband wireless USB dongles," *Electron. Lett.*, vol. 46, no. 6, pp. 388–390, Mar. 2010.
[5] T. N. Chang and J. H. Jiang, "Meandered T-shaped monopole antenna," *IEEE Trans. Antennas Propag.*, vol. 57, no. 12, pp. 3976–3978, Dec. 2009.
[6] H. Wang and M. Zheng, "Triple-band wireless local area network monopole antenna," *IET Microw. Antennas Propag.*, vol. 2, no. 4, pp. 367–372, 2008.
[7] H. Wang and M. Zheng, "An internal triple band WLAN antenna," *Antennas Wireless Propag. Lett.*, vol. 10, pp. 569–572, 2011.
[8] Q. Luo, J. R. Pereira, and H. M. Salgado, "Compact printed monopole antenna with chip inductor for WLAN," *Antennas Wireless Propag. Lett.*, vol. 10, pp. 880–883, 2011.
[9] O. Cho, H. Choi, and H. Kim, "Loop-type ground antenna using capacitor," *Electron. Lett.*, vol. 47, no. 1, pp. 11–12, Jan. 2011.
[10] Y. Liu, X. Lu, H. Choi, K.-Y. Jung, and H. Kim, "Loop-type ground antenna using resonated loop feeding, intended for mobile devices," *Electron. Lett.*, vol. 47, no. 7, pp. 426–427, Mar. 2011.
[11] Y. Liu, X. Lu, H. Choi, and H. Kim, "Excitation techniques of loop current mode of ground antenna," presented at the IEEE CSQRWT Conf., Jan. 2011.
[12] H. Choi, O. Cho, and J. Lee, "Embedded Antenna Using Ground of Terminal Device (Priority Number: 10-2010-0012775)," Korea patent application PCT/KR2010/002314.
[13] P. Vainikainen, J. Ollikainen, O. Kivekas, and I. Kelander, "Resonator based analysis of the combination of mobile handset antenna and chassis," *IEEE Trans. Antennas Propag.*, vol. 50, no. 10, pp. 1433–1444, Oct. 2002.
[14] M. Cabedo, E. Antonino, A. Valero, and M. Ferrando, "The theory of characteristic modes revisited: A contribution to the design of antennas for modern applications," *IEEE Antenna Propag. Mag.*, vol. 49, no. 5, pp. 52–68, Oct. 2007.
[15] K. L. Wong and C. H. Huang, "Printed loop antenna with a perpendicular feed for penta-band mobile phone application," *IEEE Trans. Antennas Propag.*, vol. 56, no. 7, pp. 2138–2141, Jul. 2008.
[16] Y. Li, Z. Zhang, J. Zheng, Z. Feng, and M. F. Iskander, "A compact hepta-band loop-inverted F reconfigurable antenna for mobile phone," *IEEE Trans. Antennas Propag.*, vol. 60, no. 1, pp. 389–392, Jan. 2012.
[17] Y. Liu, J. Lee, K. Jung, and H. Kim, "Dual-band PIFA using resonated loop feed structure," *Electron. Lett.*, vol. 48, no. 6, pp. 309–310, Mar. 2012.
[18] Y. Liu, J. Lee, and H. Kim, "Multi-Band Antenna Using Loop Structure," Korea patent pending 10-2012-0093542, 2012.
[19] B. S. Yarman, *Design of Ultra Wideband Antenna Matching Networks*. Berlin, Germany: Springer, 2008, ch. 5.
[20] C. T. Famdie, W. L. Schroeder, and K. Solbach, "Numerical analysis of characteristic modes on the chassis of mobile phones," presented at the Proc. EuCAP, Nov. 6–10, 2006.